

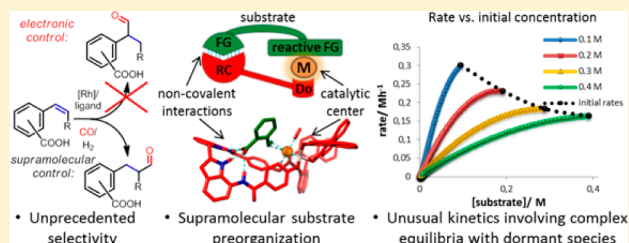
Beyond Classical Reactivity Patterns: Hydroformylation of Vinyl and Allyl Arenes to Valuable β - and γ -Aldehyde Intermediates Using Supramolecular Catalysis

Paweł Dydio, Remko J. Detz, Bas de Bruin, and Joost N. H. Reek*

van 't Hoff Institute for Molecular Sciences, University of Amsterdam, Science Park 904, 1098 XH, Amsterdam, The Netherlands

S Supporting Information

ABSTRACT: In this study, we report on properties of a series of rhodium complexes of bisphosphine and bisphosphite L1–L7 ligands, which are equipped with an integral anion binding site (the DIM pocket), and their application in the regioselective hydroformylation of vinyl and allyl arenes bearing an anionic group. In principle, the binding site of the ligand is used to preorganize a substrate molecule through noncovalent interactions with its anionic group to promote otherwise unfavorable reaction pathways. We demonstrate that this strategy allows for unprecedented reversal of selectivity to form otherwise disfavored β -aldehyde products in the hydroformylation of vinyl 2- and 3-carboxyarenes, with chemo- and regioselectivity up to 100%. The catalyst has a wide substrate scope, including the most challenging substrates with internal double bonds. Coordination studies of the catalysts under catalytically relevant conditions reveal the formation of the hydridobiscarbonyl rhodium complexes $[\text{Rh}(\text{Ln})(\text{CO})_2\text{H}]$. The titration studies confirm that the rhodium complexes can bind anionic species in the DIM binding site of the ligand. Furthermore, kinetic studies and in situ spectroscopic investigations for the most active catalyst give insight into the operational mode of the system, and reveal that the catalytically active species are involved in complex equilibria with unusual dormant (reversibly inactivated) species. In principle, this involves the competitive inhibition of the recognition center by product binding, as well as the inhibition of the metal center via reversible coordination of either a substrate or a product molecule. Despite the inhibition effects, the substrate preorganization gives rise to very high activities and efficiencies (TON > 18 000 and TOF > 6000 mol mol⁻¹ h⁻¹), which are adequate for commercial applications.



INTRODUCTION

Concern for sustainable developments sets high demands for chemical industry to make use of resources and energy with the highest possible efficiency. This pressure results in intensive research on the discovery and development of new catalytic transformations that can successfully replace stoichiometric organic reactions to create more synthetically and economically efficient routes toward high-value chemicals.¹ The general utility of a catalytic reaction depends greatly on the accessibility of active and stable catalysts that display the desired selectivity for substrates of interest, and obviously on the synthetic value of an introduced group with that transformation. The flagship example for such transformations is the hydroformylation reaction, which converts an olefinic C=C double bond into a synthetically versatile aldehyde group with 100% atom economy.^{2,3} Consequently, a variety of abundant olefins are efficiently converted to various valuable compounds, placing hydroformylation among the most important industrial processes utilizing homogeneous catalysis.⁴ However, despite intensive research in the field of hydroformylation, the regioselectivity of the reaction can be controlled only to some extent, strongly depending on substrates.^{2,3} Therefore, the technology is limited to specific classes of aldehyde compounds. For instance, β -aryl aldehydes that are key

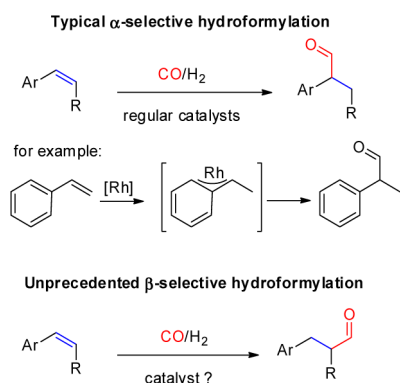
intermediates in synthesis of numerous important fine chemicals could be, in principle, obtained using hydroformylation of abundant aryl vinyls. However, the reaction typically affords only up to several percent of the β -aldehyde chemicals, alongside the main α -aldehyde products (Scheme 1).^{2,3} Therefore, the β -aryl aldehydes are usually obtained in alternative routes, involving rather sophisticated and tedious stoichiometric reactions, often burdened with production of stoichiometric amounts of the waste byproducts.⁵

In case of hydroformylation of vinyl arenes, the regioselectivity toward the α -aldehyde products originates from the formation of a rhodium α -arylalkyl intermediate that is stabilized through a π -benzyl interaction involving the aromatic ring system (Scheme 1).⁶ So far, there is no example of a catalyst that could overcome this “natural” α -selectivity for a broad scope of substrates. However, Peng and Bryant,⁷ Beller,⁸ and Zhang⁹ reported remarkable examples of catalysts that form the β -aldehyde product with a satisfactory level of selectivity, but only for styrene—the unsubstituted benchmark substrate (R = H, Ar = Ph in Scheme 1; the overall selectivities are ca. 90%, with the best regioselectivity of 96% and the

Received: March 26, 2014

Published: May 19, 2014

Scheme 1. Regioselectivity Issues in the Hydroformylation of Vinyl Arenes



chemoselectivity of 92%). In case of 1,2-disubstituted vinyl arenes ($R \neq H$, in Scheme 1), an inherently lower reactivity of an internal double bond and its possible isomerization side reactions cause that steering the selectivity to the β -position is even more troublesome.¹⁰ Currently, there is no example of the β -selective hydroformylation for such substrates. Considering the potential utility for bulk/fine chemical synthesis, catalytic systems offering such unusual selectivity are highly desired.

To generate a catalytic system that would effectively overcome the natural selectivity, we hypothesized that it is necessary to devise a catalyst that would preorganize a substrate molecule in a way that the orientation of the reactive double bond at a catalytic center favors formation of the desired isomer, at the same time hindering the reaction pathway for the usual product. In principle, such substrate preorganization can be achieved by noncovalent interactions of a directing functional group (i) with a metal center,^{11–14} or as recently shown, (ii) with a ligand of the catalyst equipped with a complementary binding site (Figure 1).^{15–19} For hydroformylation, the latter is required because the active catalyst—the neutral Rh^I complex^{2,3}—is not suited for

traditional preorganization via metal–substrate coordination, due to the excess CO present competing for substrate coordination. As a part of our ongoing efforts to exploit the potential of supramolecular chemistry for controlling the selectivity in transition metal catalysis,^{15,20} we devised catalysts in which the substrate molecules—vinyl derivatives could be preorganized using noncovalent, hydrogen bonding, interactions with a directing site of the ligand (Figure 1).²¹ Here, we report the high competence of the strategy, providing highly active and up to 100% chemo- and β -regioselective supramolecular catalysts for the hydroformylation of vinyl 2- and 3-carboxyarenes. To demonstrate the applicability of the catalytic system, we show that it can operate at temperatures between 22 and 80 °C, for a wide substrate scope and at low catalyst loadings reaching high efficiency (TON > 18 000 and TOF > 6000 mol mol⁻¹ h⁻¹). Furthermore, we show that the reactions can be performed at large scale; the products can be easily isolated and readily transformed into further valuable building blocks. Kinetic studies and in situ spectroscopic investigation give an insight into the operational mode of the most active catalyst and reveal that the catalytically active species are involved in complex equilibria involving unusual dormant (reversibly inactivated) species. Full details of these studies are presented in the following sections.²²

RESULTS AND DISCUSSION

On account of our previous studies on the development of the regioselective catalysts for hydroformylation of aliphatic olefins with anionic groups,¹⁸ we conceived of a series of catalysts with potential for the β -regioselective hydroformylation of vinyl arenes bearing a carboxyl group. Interestingly, the intended products of such transformation represent valuable intermediates in the synthesis of a series of natural products and therapeutic agents.²³ The designed catalysts comprise a bidentate ligand functionalized with (i) two phosphorus moieties for coordination to the catalytically active rhodium center^{2,3} and (ii) the diamidodiindolylmethane moiety that strongly binds to the carboxylate group²⁴ and as such serves as a substrate prebinding site. The considered bifunctional catalysts are devised to preorganize molecules of the addressed class of substrates through noncovalent binding, controlling the reaction selectivity (Figure 1b).¹⁵ The series of ligands L1–L7 (Scheme 2) represents the variation of functional, geometric, steric, and electronic properties, the influence of which is evaluated in both the catalyst structure and the catalytic performance in the hydroformylation of a series of vinylbenzoic acids.

Ligand Synthesis. The ligands are synthesized starting from easily accessible 7,7'-dinitro-2,2'-diindolomethane **1**,^{24d} which is first hydrogenated in the presence of Pd/C, to obtain diamine **2**. In one of the synthetic routes (Scheme 2), compound **2** is next reacted with phosphino carboxylic acids, following the standard condensation procedure involving a carbodiimide coupling reagent,²⁵ to give bisphosphine ligands L1–L4 in good overall yields of 62–67%.

The phosphite ligands L5–L7 are prepared following the alternative synthetic route (Scheme 2). First, the diamine **2** is reacted with benzyloxybenzoyl chlorides, in the presence of a base, to give bisamides **3a,b**. The benzyl protecting groups of **3a,b** are subsequently removed by hydrogenation in the presence of Pd/C. The reaction of the obtained diols **4a,b** with phosphorochloridites, in the presence of a base, affords phosphite ligands L5–L7 in good overall yields of 75–88%. It

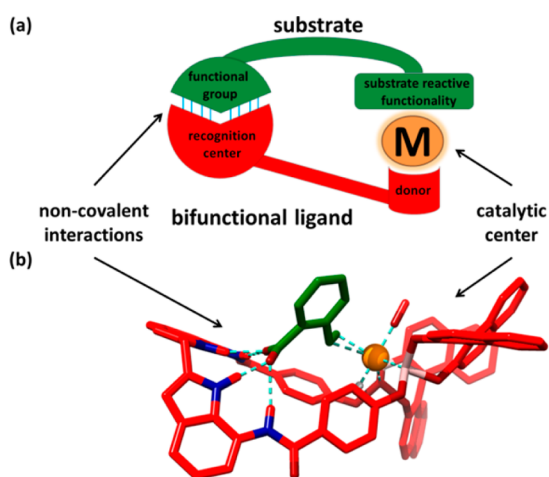
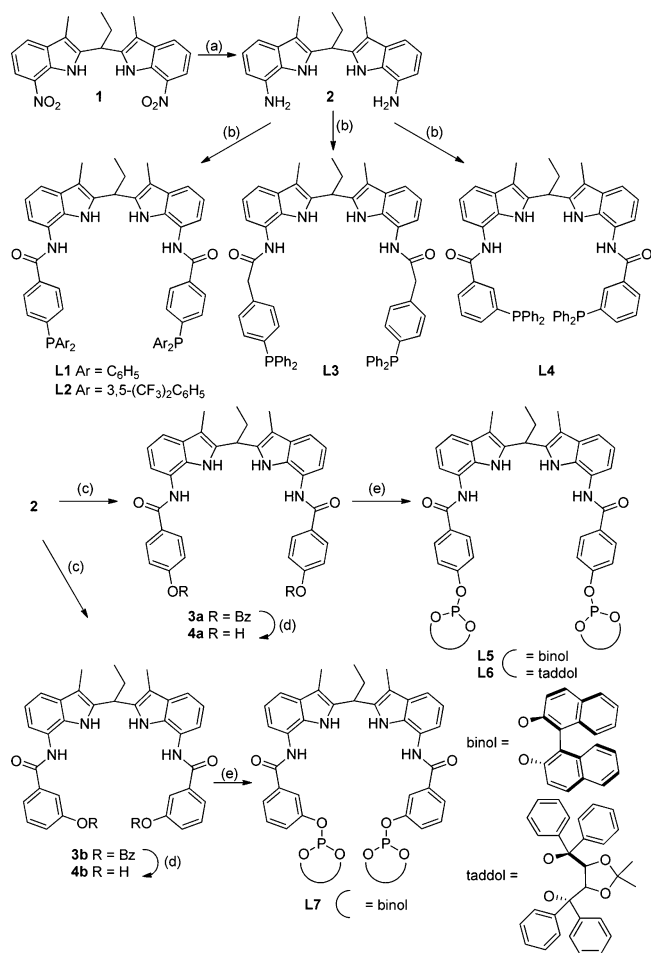


Figure 1. (a) Schematic representation of substrate preorganization by a catalyst with a bifunctional ligand, consisting of a donating function for catalytic center coordination and a specific recognition site for binding to a functional group of a substrate and (b) the molecular model (by DFT) of the hydrogen bonding-mediated preorganization of vinyl arene substrate (**S**) at the supramolecular hydroformylation catalyst of the study ($Rh(L5)$).

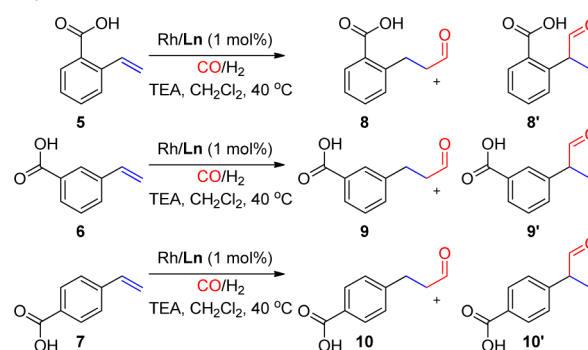
Scheme 2. Synthesis of Ligands L1–L7^a

^aReagents and conditions: (a) H₂, Pd/C, MeOH, room temperature (RT); (b) (Ar₂P)Ph(CH₂)_nCOOH (*n* = 0 or 1), diisopropylcarbodiimide (DIC), 4-dimethylaminopyridine (DMAP), 4-pyrrolidinopyridine, CH₂Cl₂, RT; (c) 3- or 4-(BzO)PhCOCl, triethylamine (TEA), CH₂Cl₂, RT; (d) H₂, Pd/C, MeOH : THF (1:3), 40 °C; (e) binol/taddol-PCl, TEA, CH₂Cl₂, -78 °C → RT. For full experimental details, see the Supporting Information (SI).

is noteworthy that the developed synthetic routes allow for simple variation of the steric, geometric, and electronic properties of ligands, if desired, by using different phosphino carboxylic acids or phosphorochloridites at the last synthetic step of the procedures.

Regioselective Hydroformylation of Vinylbenzoic Acids. We first evaluated the catalytic competence of ligands L1–L7 in the Rh-catalyzed hydroformylation of vinylbenzoic acids 5–7 (Scheme 3). In a typical experiment, the reaction is performed at 40 °C, under 20 bar of syngas (CO/H₂, 1:1) in CH₂Cl₂, with a catalyst prepared in situ (without catalyst preactivation). Importantly, for all ligands explored, the active catalysts are already formed under these mild conditions (Table 1). Pleasingly, in the case of 2-vinylbenzoic acid (5), hydroformylation using rhodium catalysts with all ligands but L3 provide β-aldehyde 8, 2-(3-oxopropane)-benzoic acid, as the major product, which is typically disfavored using regular hydroformylation catalysts. Remarkably, catalysts with ligands L5–L6 provide exclusive formation of the β-aldehyde 8, and these reactions are 100% chemo- and regioselective. Interestingly, ligands L5 and L6 also afford β-selective catalysts for

Scheme 3. Hydroformylation of 5–7 with the Rh/L1–L7 catalysts

Table 1. Evaluation of Ligands L1–L7 for the Hydroformylation of 5–7^a

ligand	substrate 5		substrate 6		substrate 7	
	% conv	% 8	% conv	% 9	% conv	% 10
L1	11	80	52	16	53	10
L2	22	85	91	32	88	18
L3	19	17	41	8	75	8
L4	50	57	87	3	74	11
L5	100	>98	100	73	100	15
L6	100	>98	94	85	64	24
L7	94	67	80	17	96	7

^aReagents and conditions: [substrate] = 0.2 M, TEA (1 equiv), [Rh(CO)₂(acac)] (1 mol %), ligands L1–L4 (1.5 mol %), ligands L5–L7 (1.1 mol %), 20 bar CO/H₂ (1:1), 40 °C, 24 h. Conversion and regioselectivity determined by ¹H NMR analysis of the reaction mixture. No side products were observed for substrates 5 and 6. Products of 7, that is, aldehydes 10 and 10' are reactive under the reaction conditions, and as observed by the ESI MS they react in the aldol condensation, lowering the chemoselectivity. For full experimental details, see the SI.

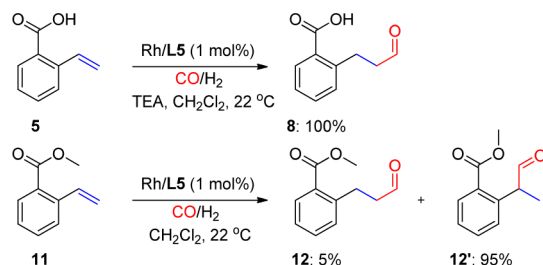
substrate 6, 3-vinylbenzoic acid, with a regioselectivity up to 85% for β-aldehyde product 9, 3-(3-oxopropane)-benzoic acid (Table 1). In turn, the last substrate from the series, that is, 4-vinylbenzoic acid (7) reacts to form the typical α-aldehyde 10' as the major product, revealing the apparent mismatch between the substrate and the supramolecular catalysts of ligands L1–L7.

We also evaluated the influence of the amount of base present in solution (triethylamine), which is used to deprotonate the substrates. We found that the reactions are slightly faster when lower amounts of base are used, with little effect on the regioselectivity (SI Table S1). Interestingly, the hydroformylation of 5 with ligands L5–L6 can be performed with substoichiometric amounts of base, retaining 100% chemo- and regioselectivity for aldehyde 8. Furthermore, the catalyst with L5 turned out to be the most active within the tested series of catalysts, leading to full substrate conversion even at room temperature.³³

Subsequently, to confirm that the supramolecular substrate–ligand interactions are responsible for the unusual selectivity, we performed a series of control experiments. A range of styrene-derivatives, with electron-withdrawing and electron-donating groups, which cannot bind to the pocket of the ligand, are hydroformylated by Rh(L5) to form the typical α-aldehyde products selectively, with only 3–10% of β-aldehydes alongside (SI Table S6). Methyl 2-vinylbenzoate (11), the ester derivative

of **5** that is its closest analogue in terms of steric and electronic properties but is unable to bind to the ligand, forms only 5% of β -aldehyde **12** and 95% of α -aldehyde **12'**. This sharp contrast in reaction selectivity for related substrates **5** and **11** demonstrates clearly the influence of preorganization effect for **5** (Scheme 4). In addition, substrate **5** reacts considerably

Scheme 4. Importance of the Supramolecular Interactions: Hydroformylation of **5 and of its Ester Analogue **11** with the Rh(L5) Catalyst^a**

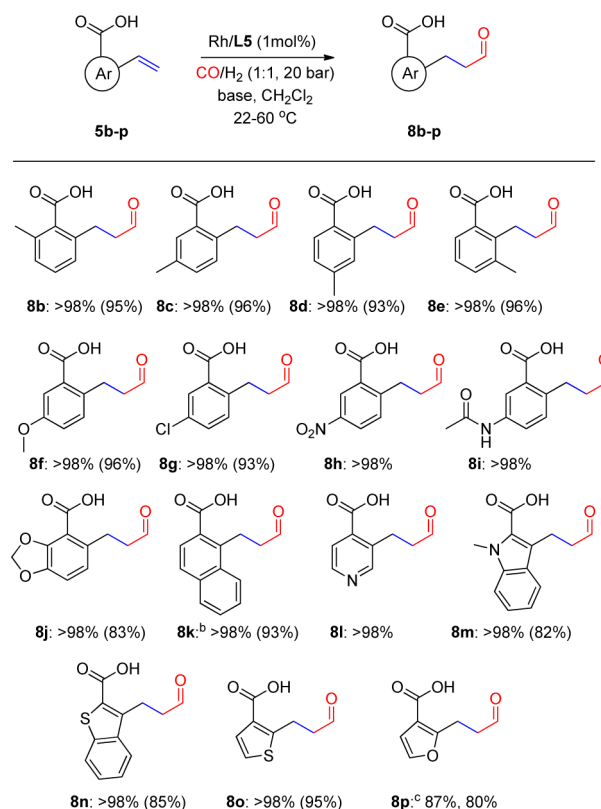


^aProduct yields were determined by NMR spectroscopy and GC analysis.

faster than its ester analogue **11** (TOF = 57.0 vs 11.7 mol mol⁻¹ h⁻¹), under otherwise similar conditions. Using the relative selectivities and overall activities for the hydroformylation of **5** and **11**, one can estimate the influence of substrate preorganization on relative rates of reaction pathways toward the α - and β -aldehyde products. Such comparison shows that the supramolecular substrate–ligand interactions result in the acceleration of the β -aldehyde formation by a factor of 60, and the deceleration of α -aldehyde formation by more than a factor of 100. These control experiments demonstrate clearly that the high activity and the unrivaled regioselectivity of Rh(L5) to form **8** stem from the substrate binding to ligand L5. For comparison, hydroformylation of **5** catalyzed by typical catalysts, i.e., rhodium complexes comprising monodentate (PPh₃, P(OPh)₃) or bidentate (xantphos and dppp; xantphos = 4,5-bis(diphenylphosphino)-9,9-dimethylxanthene, dppp = 1,3-bis(diphenylphosphino)propane) ligands, under otherwise similar conditions, do not proceed or progress with only modest activity (TOF < 9.5 mol mol⁻¹ h⁻¹), forming the α -aldehyde as the main product (with up to 6% of the β -aldehyde product alongside, with the exception of the rhodium-xantphos catalyst that forms 50% of the β -aldehyde, but with low activity of 0.2 mol mol⁻¹ h⁻¹).³³ Furthermore, the Rh-catalyst containing binol-based phosphite ligands—that is the complex resembling the Rh(L5) catalyst, but one that is not equipped with the attached anion binding pocket—shows no activity for hydroformylation of **5**, neither in the presence nor in the absence of separately added anion receptor.³³

Substrate Scope of the Catalytic System. We next evaluated the substrate scope of the supramolecular catalyst Rh(L5). Considering the high selectivity with **5**, we first focused the evaluation on a series of vinyl-2-carboxyarenes (Scheme 5). In all but one of the studied examples, the reactions form the β -aldehyde products with full regioselectivity. Most reactions were accomplished already at room temperature or slightly above, and only the reaction for naphthyl derivative **5k** required 60 °C to form the product **8k** in high yield. In general, substrates with substitutions at any position of the aryl ring are easily converted, with a broad range

Scheme 5. Substrate Scope for the Hydroformylation of Vinyl 2-Carboxyarenes **5 with the Rh(L5) Catalyst^a**



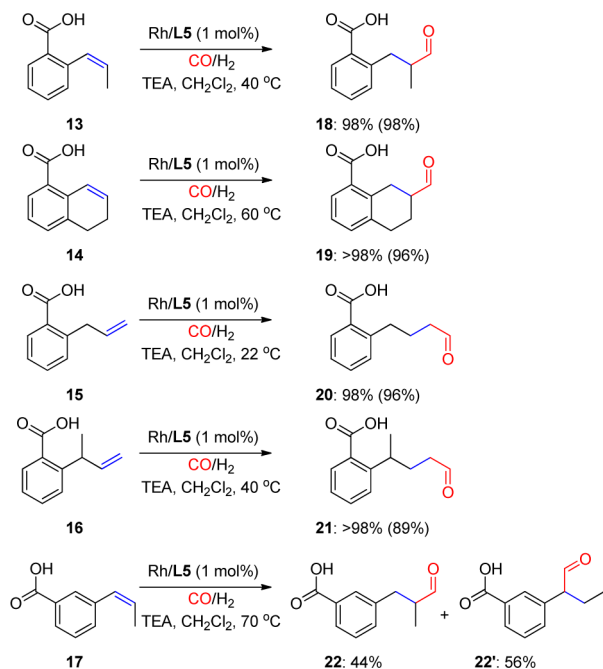
^aProduct yield and selectivity determined by ¹H and ¹³C NMR analysis of the reaction mixture. Value between parentheses indicates yield of isolated product for reactions conducted on a 0.3–0.8 mmol scale. Full conversion of the starting material in all cases (except where noted). Reagents and conditions: [**5**] = 0.2 M, base=DIPEA or TEA (0.5–1.5 equiv), [Rh(CO)₂(acac)] (1 mol %), ligand L5 (1.1 mol %), 20 bar CO/H₂ (1:1), 22–60 °C to 22–40 °C, 24–72 h. ^b95% conversion at 60 °C. ^cRegioselectivity toward aldehyde **8p** and chemoselectivity toward aldehydes, respectively. For full experimental details, see the SI.

of functional groups, such as alkyl, alkoxy, chloride, nitro, and amide groups being compatible with the catalyst. Furthermore, vinyl analogues with other aromatic and heteroaromatic rings, such as naphthyl, pyridine, indole, and (benzo)thiophene derivatives react with 100% selectivity to form the β -aldehydes. Only the reaction with furan derivative **5p** does not proceed with full selectivity, but the β -aldehyde **8p** is still formed as the major product, with 70% yield and 87% regioselectivity.

Subsequently, we evaluated even more challenging substrates with internal double bonds, i.e., β -substituted vinyl arene derivatives. In general, such substrates are significantly less reactive, and present even lower reactivity to form the β -aldehyde products.¹⁰ Besides, the double bond can isomerize, furnishing a complex mixture of isomeric products. Remarkably, catalyst Rh(L5) converts substrates **13** and **14** easily, and forms the β -aldehyde products exclusively which are isolated in nearly quantitative yield (Scheme 6).²⁶ To the best of our knowledge, these constitute the first examples of β -regioselective hydroformylation of β -substituted vinyl arene derivatives.

We also evaluated the allyl analogue of substrate **5**, that is, 2-(2-allyl)-benzoic acid (**15**). Formally, this substrate is not burdened with the reactivity issues of vinyl arenes. However,

Scheme 6. Hydroformylation of β -Substituted Vinyl and Allyl Arenes 13–17 with the Supramolecular Catalyst Rh(L5)^a



^aProduct yield determined by NMR analysis of the reaction mixture; no side products were observed. Value within parentheses indicates yield of isolated product for reactions conducted on a 0.5–0.8 mmol scale.

under hydroformylation conditions, allyl-arenes can readily isomerize to the vinyl analogues, finally resulting in the formation of mixtures of α -, β - and γ -aldehyde products.²⁷ Pleasingly, hydroformylation of substrate 15, and of its substituted analogue 16, using the Rh(L5) catalyst leads to the selective formation of the γ -aldehydes (Scheme 6).²⁸ This extends the potential application of the Rh(L5) catalyst to the synthesis of another class of building blocks, for example, for the fragrance industry.²⁹ It is noteworthy that this reveals that the catalyst has a tendency to introduce the aldehyde moiety on

the carbon atom of the double bond that is more distant from the carboxylic group. This observation is in agreement with the previously envisioned mechanistic model.^{18b}

Considering the good selectivities obtained for substrate 6, we also evaluated its analogue with the internal double bond—substrate 17 (Scheme 6). The experiments reveal that the Rh(L5) catalyst affords close to an equimolar mixture of α - and β -aldehyde products, while the catalyst with ligand L6 is poorly active for this substrate.³³

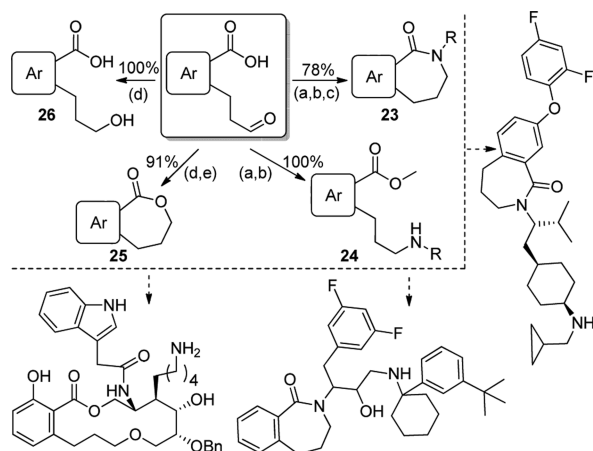
Potential for Applications. To further evaluate the application potential of the Rh(L5) catalyst, we investigated in more detail the tolerance of the catalysts to changes in the reaction conditions and its scalability (Table 2). The catalyst operates in various solvents, including dichloromethane, toluene, tetrahydrofuran (THF), and acetonitrile. Remarkably, the reaction also proceeds under ambient pressure of syngas already at room temperature, so that it can be carried out using common laboratory equipment (a Schlenk flask equipped with a balloon). Furthermore, the activity of Rh(L5) is increased by elevating the reaction temperature up to 80 °C without any loss of selectivity. This affords the high catalyst activity and efficiency (TOF > 6000 mol mol⁻¹ h⁻¹ and TON > 18 000), retaining the full reaction selectivity. This allows for applying very low catalyst loadings (0.005 mol %), which are suitable for commercial applications. Importantly, the reactions are readily scalable to multigram level (>5 g). The analytically pure product of such reaction is easily isolated in nearly quantitative yield (97%) by a straightforward acid–base extraction procedure. The β -aldehyde products are convenient synthetic building blocks, featured in synthesis of many natural products and therapeutic agents (Scheme 7).²³ We show that product 8 is easily converted in three straightforward steps (78% overall yield), through the amino aryl ester 24, to the aryl ϵ -lactam 23. Aldehyde 8 is also easily reduced to the hydroxyaryl acid 26, and subsequently reacted to form the corresponding aryl ϵ -lactone 25. These are common structural motifs of some bioactive compounds,²³ and as such, the described catalytic system affords new convenient synthetic routes toward those fine chemicals.

Coordination and Anion Binding Studies. Before exploring the mechanism by kinetic analysis, we first studied the binding properties of anions in the DIM-pocket as well as

Table 2. Evaluation of Reaction Conditions on the Hydroformylation of 5 with Rh(L5)^a

temp (°C)	time (h)	pressure (bar)	solvent	base (equiv)	Rh (mol %)	% conv	% 8
22	24	1	CH ₂ Cl ₂	1.5	1	40	>98
22	24	20	CH ₂ Cl ₂	1.5	1	100	>98
35	24	1	CH ₂ Cl ₂	1.5	1	100 ^b	>98
40	24	20	toluene	1.5	1	100	>98
40	24	20	THF	1.5	1	100	>98
40	24	20	CH ₃ CN	1.5	1	84	>98
40	24	20	CH ₂ Cl ₂	1.5	0.25	100	>98
60	24	20	CH ₂ Cl ₂	1.5	0.1	100	>98 ^c
80	1	20	CH ₂ Cl ₂	1.5	0.25	100	>98 ^c
80	1	20	CH ₂ Cl ₂	0.5	0.05	100	>98
80	1	20	CH ₂ Cl ₂	0.5	0.005	42	>98
80	12	20	CH ₂ Cl ₂	0.9	0.005	90	>98

^aReagents and conditions: [substrate] = 0.2 M, Rh(CO)₂(acac) as a rhodium source, Rh: ligand L5, 1/1.1; CO/H₂ (1/1); base = TEA (DIPEA can be used alternatively). Conversion and regioselectivity determined by ¹H NMR analysis of the reaction mixture. No side products were observed (except where noted). ^bNo full conversion in some runs, presumably due to the catalyst sensitivity and lower control of the reaction conditions at 1 bar (a balloon-based setup). ^cSmall amount (<5%) of side products present (products of the aldol condensation of 8, as identified by ESI MS). For full screening of the reaction conditions, and for full experimental details, see the SI.

Scheme 7. Transformation of Aldehyde 8 into other Valuable Building Blocks^a

^aReagents and conditions for Ar = 1,2-Ph, R = *n*-C₄H₉: (a) CH₃I, KHCO₃; (b) 1. RNH₂, 2. NaBH₄; (c) Al(CH₃)₃; (d) NaBH₄; and (e) *p*-TolSO₃H. For full experimental details, see the SI.

the coordination behavior of the various ligands to rhodium under catalytic conditions. The anion binding properties of the studied ligands are apparent from the significant downfield shift of the NH signals of both phosphine **L1** and phosphite **L5** in the ¹H NMR spectra in CD₂Cl₂ ($\Delta\delta = 2.4$ – 3.6 ppm), triggered by the presence of benzoate anions. This observation is consistent with the formation of hydrogen bonds between the NH groups of the ligands and the carboxylate group of the anion.^{24c}

The bis-coordination of the ligands to the rhodium center through the P centers is evident from the phosphorus–rhodium couplings in the ³¹P NMR spectra. For instance, **L1** and **L5** in the presence of the [Rh(acac)(C₂H₄)₂] and [Rh(acac)(CO)₂] precursors give rise to the formation of the square planar complexes—[Rh(acac)(**L1**)] and [Rh(acac)(**L5**)], respectively—the precursors of the competent hydroformylation catalysts (acac = acetylacetonate). The C_s-symmetry of phosphine ligands **L1**–**L4** is evidenced with a single doublet signal for the rhodium complexes in the ³¹P{¹H} NMR spectra.³³ In contrast, the phosphorus spectrum for [Rh(acac)(**L5**)] demonstrates the inequivalency of the P donors (Figure 2), due to the overall lack of symmetry—the C₁-symmetry of ligands **L5**–**L7** (consequences of the C_s-symmetry of the diindolylmethane core and C₂-symmetry of

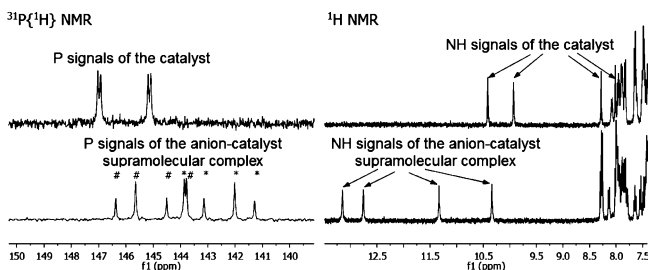


Figure 2. Fragments of ³¹P{¹H} and ¹H NMR spectra for [Rh(**L5**)(acac)] complex (0.001 M solution) in the absence (top) and the presence of PhCOO[−] anion (bottom; 1.05 equiv, in the form of TBA-PhCOO salt; TBA⁺ = tetrabutylammonium cation) measured in CD₂Cl₂; # and * denote signals of different phosphorus atoms.

the diol moieties ((*S*)-binol or (*S,S*)-taddol)). The lack of symmetry for phosphite **L5** is also revealed in the ¹H NMR spectrum, for instance, with 4 distinguishable NH signals observed (Figure 2). The NMR titration studies for [Rh(acac)(**L5**)] revealed formation of 1:1 anion-to-catalyst complexes with the benzoate, and no higher stoichiometry complexes were observed. The anion is bound strongly within the pocket of **L5** (evidenced by downfield shift of the NH signals, $\Delta\delta = 2.3$ – 3.1 ppm, Figure 2; estimated $K_a \gg 10^5$ M^{−1}, in CD₂Cl₂ based on titration studies), and does not compete effectively for the coordination site of the metal center with bidentate **L5** and acac ligands.

In Situ High-Pressure NMR and IR Analyses. The coordination properties of ligands **L1**–**L7** to the rhodium center under catalytically relevant conditions were studied using high-pressure (HP) NMR and HP infrared (IR) spectroscopic techniques. Rhodium complexes were prepared *in situ* by using [Rh(acac)(CO)₂] as the metal precursor in CD₂Cl₂ under 5 bar of syngas (H₂/CO, 1:1) for the NMR experiments, and in CH₂Cl₂ under 20 bar of syngas for the IR experiments.

Each phosphine ligand **L1**–**L4** forms nearly quantitatively³⁰ the mononuclear hydridobiscarbonyl rhodium complexes [Rh(Ln)(CO)₂H] that are generally accepted as the catalytically competent species in hydroformylation.^{2,3} The formation of the complexes is evidenced by the extensive of ¹H, ¹H{³¹P} and ³¹P{¹H} NMR spectra (Figure 3 and Table 3). The variable

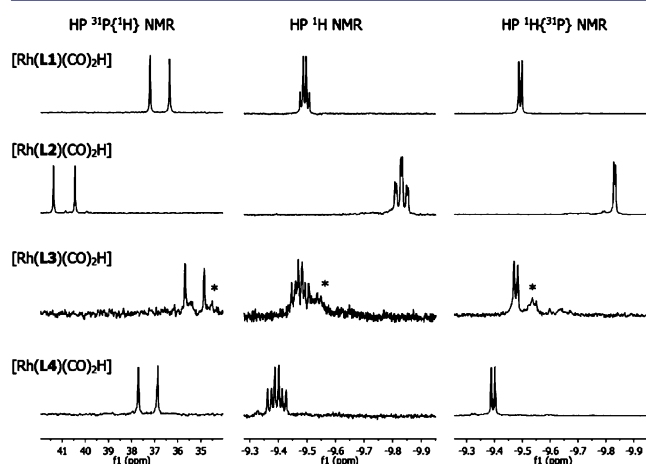


Figure 3. High pressure (HP) NMR spectra of [Rh(Ln)(CO)₂H] complexes (0.01–0.014 M solution) for phosphine ligands **L1**–**L4**, formed *in situ*, under 5 bar of syngas (CO/H₂, 1:1) measured in CD₂Cl₂; * denotes signals arising upon slow decomposition of [Rh(L3)(CO)₂H].²⁹

temperature (VT) NMR experiments allow for observation of both, the equatorial–equatorial (**ee**) and equatorial–apical (**ea**) isomers of [Rh(**L1**)(CO)₂H] at lower temperatures, that are in fast equilibrium on the NMR time scale at room temperature (rt).^{18,31,32} Small values of the phosphorus–hydride coupling at rt (Table 3) indicate that all bidentate ligands are coordinated predominantly in the **ee** fashion (the expected averaged values of ²J_{P–H} for the **ee** and **ea** are around 2 and 100 Hz, respectively).³¹

In agreement with the VT NMR study, the HP IR investigation of [Rh(**L1**)(CO)₂H] using either H₂/CO or D₂/CO (both 1:1) reveals absorption bands in the carbonyl region that correspond to the **ee** and **ea** isomeric complexes (Figure 4).^{18,33,34} The strong electron withdrawing properties

Table 3. Selected HP NMR and HP IR Data for $[\text{Rh}(\text{Ln})(\text{CO})_2\text{H}]$ of L1–L7^a

Ln	δ_{P} (ppm)	$\delta_{\text{Rh-H}}$ (ppm)	$^1J_{\text{PRh}}$ (Hz)	$^1J_{\text{PH}}$ (Hz)	$^2J_{\text{RhH}}$ (Hz)	$\nu(\text{CO})^b$ (cm^{-1})
L1	36.8	−9.50	137.5	4.1	4.4	1945, 1986, 2044
L2	40.9	−9.83	150.6	8.2	2.0	1972, 2006, 2058
L3	35.2	−9.48	134.0	9.3	5.4	1937, 1984, 2037
L4	37.3	−9.40	134.6	10.3	5.5	1943, 1986, 2043
L5 ^c	168.4 (166.9, 167.2)	−10.62 (−10.61)	−(230.4, 235.5)	−(14.1, 24.9)	−(4.7)	2021, 2050, 2077
L6	136.3	−11.09	239.7	11.6	3.5	1972, 2028, 2063
L7	171.0	−10.77				2010, 2053, 2072

^aFor experimental details, see the footnotes for Figures 2–5 and the SI. ^bOnly well-resolved absorption bands are listed. ^cValues between parentheses are measured in the mixture of $\text{CD}_3\text{CN} + \text{CD}_2\text{Cl}_2$ (1:1) – Figure 5.

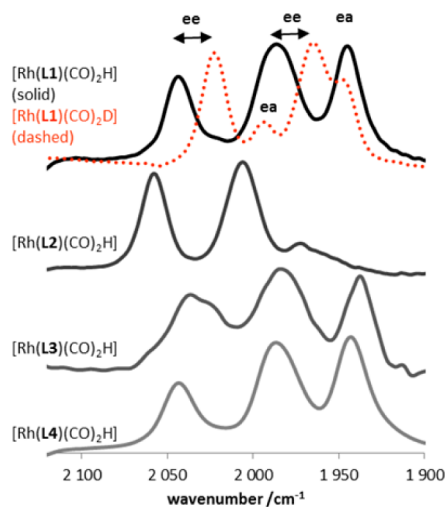


Figure 4. High pressure infrared (IR) spectra of $[\text{Rh}(\text{Ln})(\text{CO})_2\text{H}]$ complexes (0.001–0.002 M solutions) for phosphine ligands L1–L4, formed in situ, under 20 bar of syngas (CO/H_2 , 1:1; alternatively CO/D_2 , 1:1 for the deuterated species—spectrum in red) measured in CH_2Cl_2 .

of the trifluoromethyl groups significantly lower the basicity of phosphine centers of ligand L2 that further favors the ee complex geometry over the ea isomer.³¹ This is unambiguously shown by the HP IR spectrum in which the absorption bands of the ee isomer clearly dominate the spectrum (Figure 4). The VT NMR experiments show, however, that still both ee and ea isomers are present in the equilibrium. The electronic effect of the CF_3 substituents is also apparent by the shift of the absorption bands to higher wavenumbers ($\Delta\nu = 14\text{--}27\text{ cm}^{-1}$), due to the lowered electron density on the metal, and hence, decrease in back-bonding from the rhodium to the carbonyl ligand. In contrast, the electron donating methylene groups of ligand L3 shift the bands to lower wavenumbers ($\Delta\nu = -2\text{--}8\text{ cm}^{-1}$; Figure 4). Ligand L4 forms a hydridobiscarbonyl rhodium complex $[\text{Rh}(\text{L4})(\text{CO})_2\text{H}]$ that is electronically similar to the one formed with its structural isomer, ligand L1, as evidenced by HP NMR and HP IR studies (Table 3, Figures 3 and 4). Notably, the HP IR studies for all phosphine ligands L1–L4, performed under actual hydroformylation conditions, indicate a quantitative precatalyst activation process that even at room temperature takes less than 2 h. Furthermore, the complexes formed are stable under the catalytic conditions.²⁹

The studies for phosphite ligands show that the rhodium complex formed with ligand L5 displays a clear hydride signal at -10.62 in the ^1H NMR spectrum in CD_2Cl_2 . However, both the proton and phosphorus NMR spectra present broad signals,

also during the VT experiments (25 to $-95\text{ }^\circ\text{C}$), which do not allow for a straightforward analysis of the complex structure. To exclude the formation of complexes of different stoichiometries (e.g., clusters), we performed a diffusion NMR (DOSY) experiment. The obtained diffusivity indicates formation of only one discrete complex with a hydrodynamic radius of about 9.4 \AA , which is similar to that determined for $[\text{Rh}(\text{L6})(\text{CO})_2\text{H}]$ (7.7 \AA ; vide infra), and corresponds most closely to $[\text{Rh}(\text{L5})(\text{CO})_2\text{H}]$, as determined by the computational model.³³ Furthermore, the HP IR reveals only vibrations for terminal CO ligands, and no signals in the bridging CO region ($1800\text{--}1900\text{ cm}^{-1}$) can be detected. Fortunately, the complex shows the well-resolved signals in the NMR spectra of samples recorded in a 1:1 mixture of CD_2Cl_2 and CD_3CN , that confirms the structure of $[\text{Rh}(\text{L5})(\text{CO})_2\text{H}]$ (Figure 5). The values of P–

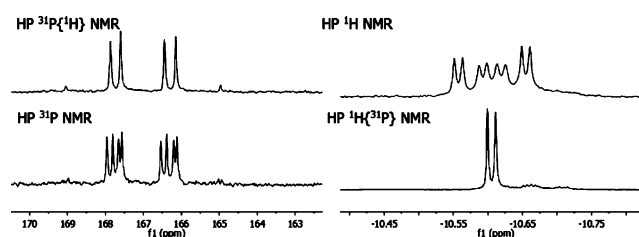


Figure 5. High pressure (HP) NMR spectra of $[\text{Rh}(\text{L5})(\text{CO})_2\text{H}]$ complex (0.02 M solution), formed in situ, under 5 bar of syngas (CO/H_2 , 1:1) measured in $\text{CD}_3\text{CN} + \text{CD}_2\text{Cl}_2$ (1:1).

H couplings indicate that the hydride $[\text{Rh}(\text{L5})(\text{CO})_2\text{H}]$ complex exists as a mixture of ee and ea conformations, with a predominance of the former. The HP IR presents the vibrations typical for both ee and ea conformations (yet some bands overlap, Figure 6).³⁰

Ligand L6 forms the hydridobiscarbonyl rhodium complex $[\text{Rh}(\text{L6})(\text{CO})_2\text{H}]$, as evidenced by the HP NMR spectra recorded in CD_2Cl_2 (Figure 7 and Table 3). Alike for other ligands, the value of P–H coupling indicates a dynamic equilibrium between ee and ea complexes, with a predominance of the ee complex.^{30,31} The VT NMR analysis shows that the fluxionality is not halted completely even at $-95\text{ }^\circ\text{C}$, which suggests low-energy-barriers for Berry pseudorotations between the conformations.³⁰ In line with the NMR studies, the HP IR analysis shows signals corresponding to both the ee and ea complexes (Figure 6).³⁰

Finally, the rhodium complex of ligand L7 shows a clear hydride signal at -10.77 on the ^1H NMR spectrum in CD_2Cl_2 . However, similarly to the complex of L5, the signals at the NMR spectra are broad, even when measured in a mixture of CD_2Cl_2 and CD_3CN , hampering the analysis. The HP IR reveals the presence of the absorption bands typical for ee

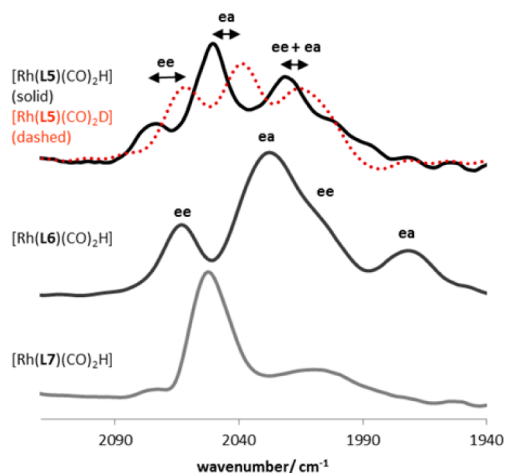


Figure 6. High pressure infrared (IR) spectra of $[\text{Rh}(\text{Ln})(\text{CO})_2\text{H}]$ complexes (0.001–0.002 M solutions) for phosphite ligands L5–L7, formed in situ, under 20 bar of syngas (CO/H_2 , 1:1; alternatively CO/D_2 , 1:1 for the deuterated species—spectrum in red) measured in CH_2Cl_2 ; the assignment of the signals was verified with DFT calculations.

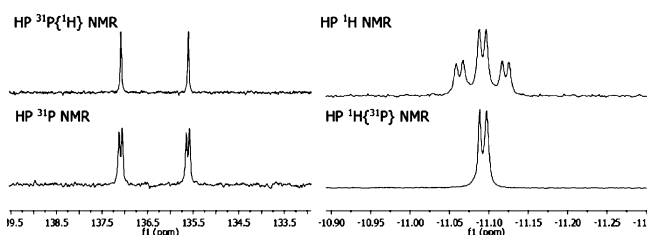


Figure 7. High pressure (HP) NMR spectra of $[\text{Rh}(\text{L6})(\text{CO})_2\text{H}]$ complex (0.014 M solution), formed in situ, under 5 bar of syngas (CO/H_2 , 1:1) measured in CD_2Cl_2 .

conformations of the hydridobiscarbonyl rhodium complexes, however, formation of other complexes cannot be excluded (Figure 6).

Mechanistic Investigation. To gain a deeper insight into this supramolecular catalytic system, we studied the hydroformylation reactions by $\text{Rh}(\text{L5})$ in more detail with kinetic experiments and further in situ spectroscopy.

Kinetic Studies. Reaction progress kinetic analysis³⁵ for the hydroformylation of **5** with $\text{Rh}(\text{L5})$ (monitored by gas-uptake under standard conditions: CO/H_2 1:1, 22 bar (constant), 30 °C; with catalyst preactivation), provided further insight in the reaction mechanism. First, experiments at different catalyst concentrations (0.0005–0.002 M of Rh) reveal first-order kinetics in $\text{Rh}(\text{L5})$,³³ in line with the mononuclear structure of the active catalyst. Interestingly, experiments at different initial substrate concentrations (0.1–0.4 M of **5**) reveal a contribution of two competing equilibria preceding the rate-determining step of the catalytic cycle. For each individual experiment, the rate of the reaction progressively slows down as a result of substrate consumption as the reaction proceeds, thus indicating an overall positive rate dependence in **5** (~ 0.75 – 1.0 rate order in **5**, Figure 8). However, the reactions also substantially slow down upon increasing the total (initial) substrate concentration (nonlinear negative dependence of the initial rate in **5**, black dashed curve in Figure 8). In fact, further experiments show that adding the product or a different carboxylate-containing compound to the initial reaction mixture slows down the

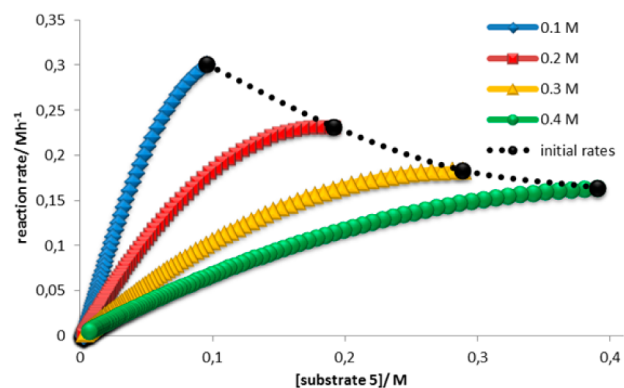


Figure 8. Graphical representation of the kinetic profiles: reaction rate versus substrate concentration plots from reactions at different initial substrate concentration for hydroformylation of **5** with the $\text{Rh}/\text{L5}$ catalyst, determined by gas uptake methods. Reagents and conditions: 22 bar CO/H_2 (1:1), 30 °C, CH_2Cl_2 , $c(\text{Rh}) = 0.001$ M, $[\text{Rh}(\text{CO})_2(\text{acac})]/\text{L5} = 1:1.1$; TEA (1.5 equiv of **5**). Incubation time for the precatalyst activation = ca. 20 h. For full experimental details, see the SI.

reaction as well (vide infra, Figure 9). Therefore, in principle, the reaction rates reveal a negative rate dependence on the total carboxylate concentration, which includes both the substrate and the product.

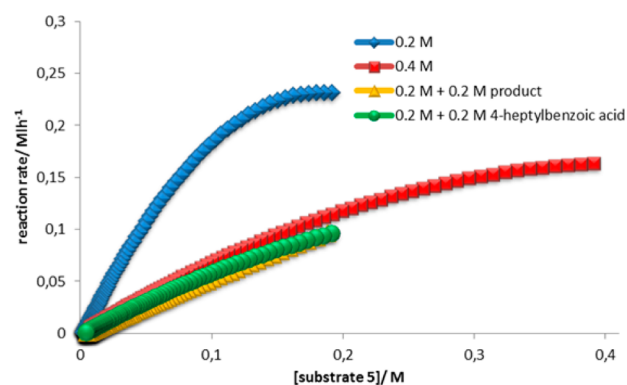


Figure 9. Graphical representation of the kinetic profiles: reaction rate versus substrate concentration plots from reactions at different initial substrate concentration and in the presence or absence of the product or 4-heptylbenzoic acid, for hydroformylation of **5** with the $\text{Rh}/\text{L5}$ catalyst, determined by gas uptake methods. Reagents and conditions: 22 bar CO/H_2 (1:1), 30 °C, CH_2Cl_2 , $c(\text{Rh}) = 0.001$ M, $[\text{Rh}(\text{CO})_2(\text{acac})]/\text{L5} = 1:1.1$; TEA (1.5 equiv of **5** + additive). Incubation time for the precatalyst activation = ca. 20 h. For full experimental details, see the SI.

It has been previously reported that carboxylic acid additives can have an inhibiting effect on the hydroformylation of 1-hexene,³⁶ but we have not encountered this for our phosphine-based complexes.^{18b} Considering the relatively high electrophilicity of the rhodium center of phosphite-based complexes (as compared to phosphine based systems), the carboxylate group of a substrate can coordinate to the rhodium center, next to the proposed binding in the recognition site of **L5**. Therefore, the double bond of prebound substrate competes for the metal coordination site with the carboxylate groups of other molecules that are present in solution, which thus can effectively slow down the reaction.

To assess the possibility of progressive catalyst deactivation in the course of the reaction, which would affect the observed reaction rate dependences, and to evaluate the influence of the product on the reaction rate, we performed the following series of kinetic experiments: (A) reaction with a 0.4 M substrate concentration, (B) reaction with a mixture of 0.2 M of the substrate and 0.2 M of the product (8), that is simulating experiment A at 50% substrate conversion; and (C) reaction with a 0.2 M substrate concentration (without product addition).³⁴ Experiments A and B indicate that the catalyst is quite stable in this reaction time window (50% conversions within ~0.5–1.5 h), as the plots of reaction rate in substrate concentration overlay reasonably well (red and yellow curves, Figure 9).³⁷ Experiments B and C clearly show that the reaction rate is indeed inhibited by the product (yellow versus blue curves, Figure 9). Moreover, 4-heptylbenzoic acid that is electronically similar to the product yet devoid of the aldehyde function imposes the same influence on the reaction rate (experiment D, Figure 9). This unambiguously shows that the carboxylic group is responsible for the catalyst inhibition.

As the product is able to bind to the recognition center of **LS**, it may affect the reaction rates after partial substrate conversion through competition with the substrate for the binding to **Rh(LS)**. Such product–substrate competition effect was detected before for a related reaction.^{18b} For the current system, considering the same total concentration of species having a carboxylate moiety in experiments A and B, the metal center is inhibited by the carboxylate coordination to the same extent. At this level of concentrations and with high K_a ($>10^5$ M^{-1}), the recognition center of **LS** is almost fully occupied by the substrate (or any carboxylate-containing compound). Therefore, the lower initial reaction rate for experiment B than for A results directly from competition of the product with the substrate for binding to the recognition center of **Rh(LS)**. Such competitive product inhibition is in line with the devised enzyme-type mechanism in which the substrate prebinds to the recognition center of **Rh(LS)** prior the alkene coordination and conversion at the metal center.³⁸

In Situ Spectroscopic Studies. To gain a deeper insight into the complexes of **Rh(LS)** formed during the catalytic reaction, we performed a series of in situ HP NMR and IR experiments. The $^{31}P\{^1H\}$ NMR spectrum recorded for the hydroformylation of ester **11** shows only signals corresponding to $[Rh(LS)(CO)_2H]$ (Figure 10), revealing that the rhodium hydride species is the resting state of **Rh(LS)**. The study with substrate **5** is hampered due to broad signals in both proton

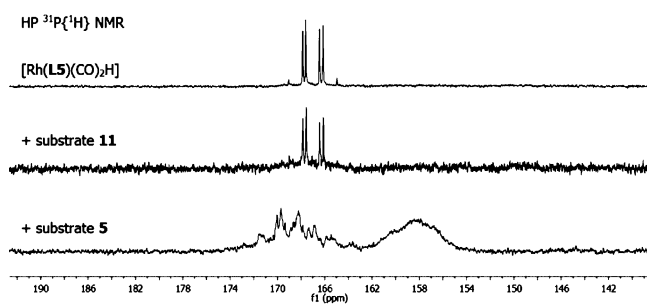


Figure 10. High pressure $^{31}P\{^1H\}$ NMR spectra of **Rh(LS)** complexes (0.01 M solution) in the absence (above) and in the presence of 10 equiv of substrate **11** (middle) or substrate **5** (below) and 15 equiv of TEA, formed in situ, under 5 bar of syngas (CO/H_2 , 1:1) measured in $CD_3CN + CD_2Cl_2$ (1:1).

and phosphorus NMR spectra. However, the data shows the formation of a mixture of complexes, indicated by the signals at 158 and 168 ppm in the $^{31}P\{^1H\}$ NMR spectrum (Figure 10), and by the hydride signal at -10.72 ppm (at substoichiometric amount) in the 1H NMR spectrum, when measured in a $CD_3CN + CD_2Cl_2$ mixture. The $^{31}P\{^1H\}$ NMR studies in CD_3CN reveal in addition a complex with a set of well-resolved signals—two doublets of doublets centered at 180.1 and 181.2 ppm, with $^1J_{Rh-P} = 286$ and 288 Hz, respectively, and with $^2J_{P1-P2} = 25$ Hz (Figure 11). The proton-coupled ^{31}P NMR

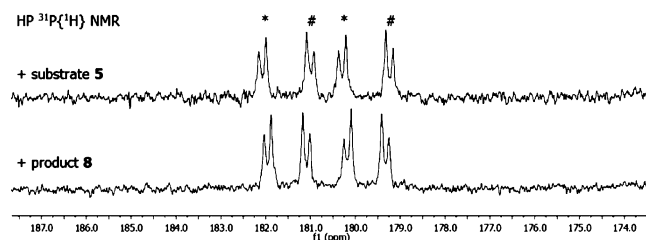


Figure 11. Fragments of high pressure $^{31}P\{^1H\}$ NMR spectra of **Rh(LS)** complexes (0.01 M solution) in the presence of 10 equiv of substrate **5** (above) or product **8** (below) and 15 equiv of TEA, formed in situ, under 5 bar of syngas (CO/H_2 , 1:1) measured in CD_3CN ; # and * denote signals of different phosphorus atoms.

spectrum shows no coupling with the hydride signals for this complex. The characteristics can be assigned to a square planar complex with cis ligand coordination, such as $[(RCO_2)Rh(LS)(CO)]$, in line with the coordination of carboxylate species to the metal center anticipated from the results of the kinetic experiments. In fact, the formation of related complexes (e.g., $[(RCO_2)Rh(PPh_3)_2(CO)]$) in the presence of carboxylic acids was reported before.^{17a,36} Such complexes were found to be in equilibrium with the rhodium hydride species,^{36a} and thus represent the dormant state of the catalyst. The experiment for **Rh(LS)** with product **8** shows the same mixture of complexes on the $^{31}P\{^1H\}$ NMR spectrum (Figure 11). Thus, the double bond of **5** is not involved directly in the formation of the new complexes. Moreover, similar spectra are recorded also with different acids, such as 4-heptylbenzoic acid and benzoic acid.³⁴ The small shifts of the signals show that the complex is somewhat affected by the electronic properties of the acid, being in agreement with the carboxylate coordination.^{36,39}

The in situ HP IR spectroscopy also shows that $[Rh(LS)(CO)_2H]$ partially turns into different species in the presence of substrate **5**, as indicated by two additional strong and broad bands at 1901 and 1999 cm^{-1} . No characteristic acyl band at ~ 1675 – 1690 cm^{-1} was detected that could indicate the formation of the acyl complex $[RC(O)Rh(LS)(CO)_2]$ representing the alternative resting state of the catalyst (Type II kinetics).^{33,40} Upon reaching full substrate conversion, the spectrum does not revert to $[Rh(LS)(CO)_2H]$, as expected for the acyl complex.³⁹ Furthermore, the IR spectrum of **Rh(LS)** in the presence of product **8** (without any substrate) indicates formation of the same species (bands at 1901 and 1999 cm^{-1}).³⁴ Besides, according to IR, the catalyst forms similar complexes in the presence of 4-heptylbenzoic acid (with the additional bands at 2000 and 1900 cm^{-1}). The findings clearly show that the carboxylate group is involved in the formation of the new species that represent the additional dormant state of the catalyst.³⁶

Taking all of the above results together, the findings reveal the events taking place on the catalyst (Figure 12). First, the

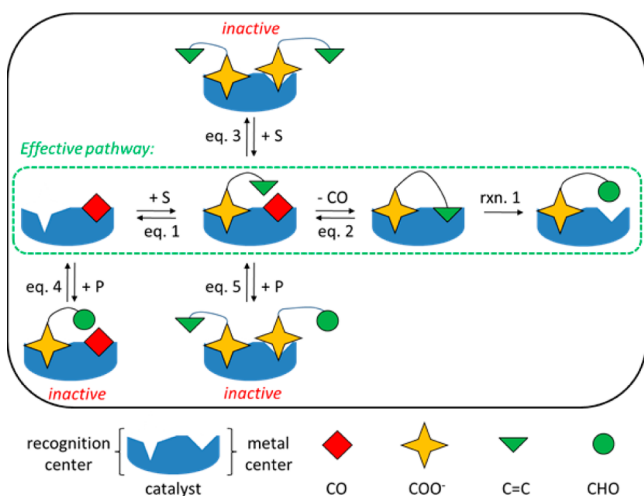


Figure 12. Simplified mechanism for hydroformylation of substrates bearing a carboxylate moiety with catalyst Rh(LS), including putative equilibria and reversible catalyst inhibition.

substrate molecule (S) binds via the carboxylate group to the recognition site of the catalyst (Cat.)—eq 1. Once the CO dissociates from the rhodium center, either (i) the double bond of the prebound substrate coordinates—eq 2—and is converted to the aldehyde followed by the product release—rxn. 1; or (ii) the carboxylate group of another (free) substrate molecule coordinates—eq 3—forming inactive complex reversibly. After product formation and release, the catalyst binds another substrate molecule, or alternatively it binds the product (P) in the recognition center—eq 4. The latter represents the classic competitive reversible product inhibition.^{18b,38} Besides, the product formed can also coordinate to the rhodium center, once CO dissociates—eq 5.

CONCLUSIONS

We demonstrate in this work that bifunctional catalysts that are equipped with a catalytic center and an integral anion binding site (the DIM pocket) afford unprecedented reversal of selectivity to form otherwise disfavored products in the hydroformylation of vinyl 2- and 3-carboxyarenes, with chemo- and regioselectivities up to 100%. The catalyst proved to be selective for a wide scope of substrates, including the most challenging substrates with an internal double bond. In addition to the unusual regioselectivity, the supramolecular substrate preorganization gives rise to very high activities and efficiencies. The kinetic studies and in situ spectroscopy reveal that the active species of Rh(LS) is involved in complex equilibria including dormant species. In principle, this involves the competitive inhibition of the recognition center by product binding, as well as the inhibition of the metal center via reversible coordination of either a substrate or a product. Overall, this results in the efficient formation of the desired product, despite the unusual substrate inhibition effects. Considering the unprecedented reactivity and that many transition metal catalyzed processes involve elementary steps similar to those of the reaction of this work, the explored supramolecular methodology should assist in the development of other selective transformations in chemical catalysis. This

should contribute to the development of new, sustainable methods for the synthesis of important fine chemicals. Research along these lines is continued in our laboratories.

ASSOCIATED CONTENT

Supporting Information

Details concerning materials and methods, catalytic and kinetic studies, coordination and binding studies, DFT studies, experimental procedures, and spectral data for new compounds (including images of NMR spectra). This material is available free of charge via the Internet at <http://pubs.acs.org>.

AUTHOR INFORMATION

Corresponding Author

j.n.h.reek@uva.nl

Notes

The authors declare no competing financial interest.

ACKNOWLEDGMENTS

We kindly acknowledge the NRSC-C and the NWO for financial support, and Dr. J. I. van der Vlugt and Dr. W. I. Dzik for helpful discussions and valuable suggestions.

REFERENCES

- (1) Beller, M. *Chem. Soc. Rev.* **2011**, *40*, 4891–4892.
- (2) van Leeuwen, P. W. N. M.; Claver, C. *Rhodium Catalyzed Hydroformylation*; Kluwer Academic Publishers: Dordrecht, 2000.
- (3) (a) Franke, R.; Selent, D.; Börner, A. *Chem. Rev.* **2012**, *112*, 5675–5732. (b) Breit, B.; Seiche, W. *Synthesis* **2001**, *2001*, 1–36.
- (4) (a) Cornils, B.; Herrmann, W. A., Eds. *Applied Homogeneous Catalysis with Organometallic Compounds: A Comprehensive Handbook in Three Vols.*, 2nd ed.; Wiley-VCH: Weinheim, 2002. (b) Beller, M.; Bolm, C., Eds. *Transition Metals for Organic Synthesis*; Wiley-VCH: Weinheim, 2004.
- (5) (a) Duerfeldt, A. S.; Brandt, G. E. L.; Blagg, B. S. J. *Org. Lett.* **2008**, *11*, 2353–2356. (b) Spletstoser, J. T.; White, J. M.; Rao Tunoori, A.; Georg, G. I. *J. Am. Chem. Soc.* **2007**, *129*, 3408–3419.
- (c) Colbon, P.; Ruan, J.; Purdie, M.; Mulholland, K.; Xiao, J. *Org. Lett.* **2011**, *13*, 5456–5459.
- (6) (a) van Leeuwen, P. W. N. M.; Claver, C. *Rhodium Catalyzed Hydroformylation*; Kluwer Academic Publishers: Dordrecht, 2000; pp 29–31. (b) Yu, S.; Chie, Y.; Guan, Z.; Zou, Y.; Li, W.; Zhang, X. *Org. Lett.* **2009**, *11*, 241–244. (c) Nelsen, E. R.; Landis, C. R. *J. Am. Chem. Soc.* **2013**, *135*, 9636–9639.
- (7) Peng, W.-J.; Bryant, D. R. (UCC) PCT Int. Patent WO 03/78444, 2003.
- (8) Jennerjahn, R.; Piras, I.; Jackstell, R.; Franke, R.; Wiese, K.-D.; Beller, M. *Chem.—Eur. J.* **2009**, *15*, 6383–6388.
- (9) Cai, C.; Yu, S.; Cao, B.; Zhang, X. *Chem.—Eur. J.* **2012**, *18*, 9992–9998.
- (10) (a) van Leeuwen, P. W. N. M.; Roobeek, C. F. *J. Organomet. Chem.* **1983**, *258*, 343–350. (b) van Leeuwen, P. W. N. M.; Claver, C. *Rhodium Catalyzed Hydroformylation*; Kluwer Academic Publishers: Dordrecht, 2000; pp 55–59.
- (11) Daugulis, O.; Do, H.-Q.; Shabashov, D. *Acc. Chem. Res.* **2009**, *42*, 1074–1086 and references therein.
- (12) Chen, X.; Engle, K. M.; Wang, D.-H.; Yu, J.-Q. *Angew. Chem., Int. Ed.* **2009**, *48*, 5094–5115.
- (13) Leow, D.; Li, G.; Mei, T.-S.; Yu, J.-Q. *Nature* **2012**, *486*, 518–522.
- (14) Wang, D.-H.; Engle, K. M.; Shi, B.-F.; Yu, J.-Q. *Science* **2010**, *327*, 315–319.
- (15) For review, see: Dydio, P.; Reek, J. H. N. *Chem. Sci.* **2014**, *5*, 2135–2145.
- (16) For key examples, see: Das, S.; Incarvito, C. D.; Crabtree, R. H.; Brudvig, G. W. *Science* **2006**, *312*, 1941–1943.

(17) (a) Smejkal, T.; Gribkov, D.; Geier, J.; Keller, M.; Breit, B. *Chem.—Eur. J.* **2010**, *16*, 2470–2478. (b) Smejkal, T.; Breit, B. *Angew. Chem., Int. Ed.* **2008**, *47*, 311–315.

(18) (a) Dydio, P.; Dzik, W. I.; Lutz, M.; de Bruin, B.; Reek, J. H. N. *Angew. Chem., Int. Ed.* **2011**, *50*, 396–400. (b) Dydio, P.; Detz, R. J.; Reek, J. H. N. *J. Am. Chem. Soc.* **2013**, *135*, 10817–10828. (c) Dydio, P.; Ploeger, M.; Reek, J. H. N. *ACS Catal.* **2013**, *3*, 2939–2942. (d) Dydio, P.; Reek, J. H. N. *Nat. Protoc.* **2014**, *9*, 1183–1191.

(19) (a) Fackler, P.; Berthold, C.; Voss, F.; Bach, T. *J. Am. Chem. Soc.* **2010**, *132*, 15911–15913. (b) Fackler, P.; Huber, S. M.; Bach, T. *J. Am. Chem. Soc.* **2012**, *134*, 12869–12878.

(20) Meeuwissen, J.; Reek, J. H. N. *Nat. Chem.* **2010**, *2*, 615–621.

(21) For an interesting alternative approach, developed by the groups of Grünanger and Breit, and Tan and co-workers, using reversible covalent bonding of catalytic ligand-like directing groups, see: (a) Grünanger, C. U.; Breit, B. *Angew. Chem., Int. Ed.* **2008**, *47*, 7346–7349. (b) Grünanger, C. U.; Breit, B. *Angew. Chem., Int. Ed.* **2010**, *49*, 967–970. (c) Lightburn, T. E.; Dombrowski, M. T.; Tan, K. L. *J. Am. Chem. Soc.* **2008**, *130*, 9210–9211. (d) Worthy, A. D.; Gagnon, M. M.; Dombrowski, M. T.; Tan, K. L. *Org. Lett.* **2009**, *11*, 2764–2767. (e) Sun, X.; Frimpong, K.; Tan, K. L. *J. Am. Chem. Soc.* **2010**, *132*, 11841–11843. (f) Lightburn, T. E.; De Paolis, O. A.; Cheng, K. H.; Tan, K. L. *Org. Lett.* **2011**, *13*, 2686–2689. For the parent approach, using stoichiometric amounts of covalently bound auxiliary ligand-like directing groups, see ref 21l and key examples: (g) Jackson, W. R.; Perlmutter, P.; Tasdelen, E. E. *J. Chem. Soc. Chem. Commun.* **1990**, 763–764. (h) Leighton, J. L.; O’Neil, D. N. *J. Am. Chem. Soc.* **1997**, *119*, 11118–11119. (i) Krauss, I. J.; Wang, C. C.-Y.; Leighton, J. L. *J. Am. Chem. Soc.* **2001**, *123*, 11514–11515. (j) Breit, B.; Breuninger, D. *J. Am. Chem. Soc.* **2004**, *126*, 10244–10245. (k) Breit, B.; Grünanger, C. U.; Abillard, O. *Eur. J. Org. Chem.* **2007**, *2007*, 2497–2503. For review on removable directing groups in organic synthesis and catalysis, see: (l) Rousseau, G.; Breit, B. *Angew. Chem., Int. Ed.* **2011**, *50*, 2450–2494 and references therein.

(22) Preliminary results of these studies have been communicated: Dydio, P.; Reek, J. H. N. *Angew. Chem., Int. Ed.* **2013**, *52*, 3878–3882.

(23) (a) Hiraiwa, Y.; Morinaka, A.; Fukushima, T.; Kudo, T. *Bioorg. Med. Chem. Lett.* **2009**, *19*, 5162–5165. (b) Duerfeldt, A. S.; Peterson, L. B.; Maynard, J. C.; Ng, C. L.; Eletto, D.; Ostrovsky, O.; Shinogle, H. E.; Moore, D. S.; Argon, Y.; Nicchitta, C. V.; Blagg, B. S. *J. Am. Chem. Soc.* **2012**, *134*, 9796–9804. and references therein. (c) Deadman, J. J.; Jones, E. D.; Le, T. G.; Rhodes, D. I.; Thienthong, N.; van de Graff, N. A.; Winefield, L. J. PCT Int. Patent WO 2010/000031, 2010. (d) John, V.; Maillard, M.; Tucker, J.; Aquino, J.; Jagodzinska, B.; Proget, L.; Tung, J.; Bowers, D.; Dressen, D.; Probst, G.; Shah, N. PCT Int. Patent WO 2005/087751, 2005. (e) Pfefferkorn, J. A.; Choi, C.; Song, Y.; Trivedi, B. K.; Larsen, S. D.; Askew, V.; Dillon, L.; Hanselman, J. C.; Lin, Z.; Lu, G.; Robertson, A.; Sekerke, C.; Auerbach, B.; Pavlovsky, A.; Harris, M. S.; Bainbridge, G.; Caspers, N. *Bioorg. Med. Chem. Lett.* **2007**, *17*, 4531–4537. (f) Zhou, J.; Matos, M.-C.; Murphy, P. V. *Org. Lett.* **2011**, *13*, 5716–5719. and references therein. (g) Mihalic, J. T.; Kim, Y.-J.; Lizarzaburu, M.; Chen, X.; Deignan, J.; Wanska, M.; Yu, M.; Fu, J.; Chen, X.; Zhang, A.; Connors, R.; Liang, L.; Lindstrom, M.; Ma, J.; Tang, L.; Dai, K.; Li, L. *Bioorg. Med. Chem. Lett.* **2012**, *22*, 2046–2051 and references therein.

(24) (a) Dydio, P.; Zieliński, T.; Jurczak, J. *Chem. Commun.* **2009**, *45*, 4560–4562. (b) Dydio, P.; Zieliński, T.; Jurczak, J. *Org. Lett.* **2010**, *12*, 1076–1078. (c) Jurczak, J.; Chmielewski, M. J.; Dydio, P.; Lichosyt, D.; Ulatowski, F.; Zieliński, T. *Pure Appl. Chem.* **2011**, *83*, 1543–1554. (d) Dydio, P.; Lichosyt, D.; Zieliński, T.; Jurczak, J. *Chem.—Eur. J.* **2012**, *18*, 13686–13701. For a review, see: (e) Dydio, P.; Lichosyt, D.; Jurczak, J. *Chem. Soc. Rev.* **2011**, *40*, 2971–2985.

(25) Izdebski, J.; Kunce, D. *J. Pept. Sci.* **1997**, *3*, 141–144.

(26) Although both the ligand and the aldehyde products are chiral, there was no enantioselectivity observed in these reactions.

(27) Axet, M. R.; Castillon, S.; Claver, C. *Inorg. Chim. Acta* **2006**, *359*, 2973–2979.

(28) For comparison, hydroformylation of substrates **15** and **16** catalyzed by a rhodium catalyst using PPh₃ as a phosphorus ligand,

under otherwise identical conditions, furnishes expected mixtures of γ - and β -aldehydes with ratios of 74:26 and 76:24, respectively (at 56% and >99% conversion, respectively). Again, the presence of separately added anion receptor negligibly changes the outcome of these reactions (providing a mixtures of γ - and β -aldehydes with ratios of 76:24 and 78:22, with 52% and >99% conversion, for **15** and **16**, respectively). Furthermore, hydroformylation of methyl ester analogues of **15** and **16**—the substrates that do not bind to the recognition center of L5—catalyzed by the Rh/L5 catalyst also affords mixtures of γ - and β -aldehydes with ratios of 62:38 and 73:27, respectively, (at full substrate conversion). These experiments confirm the importance of the noncovalent interactions in controlling the selectivity of hydroformylation of allyl arene derivatives.

(29) Saudan, L. *Acc. Chem. Res.* **2007**, *40*, 1309–1319.

(30) At the relatively high NMR concentration, and low pressure of syngas (5 bar of CO/H₂), the complex of ligand L3 is slowly decomposing, however, as indicated by the HP IR studies, it seems to be more stable at the catalytic conditions.

(31) (a) van Rooy, A.; Kamer, P. C. J.; van Leeuwen, P. W. N. M.; Goubitz, K.; Fraanje, J.; Veldman, N.; Spek, A. L. *Organometallics* **1996**, *15*, 835–847. (b) Buisman, G. J. H.; Vos, E. J.; Kamer, P. C. J.; van Leeuwen, P. W. N. M. *J. Chem. Soc., Dalton Trans.* **1995**, 409–417.

(32) For the NMR studies of a mixture of ee and ea complexes, see: (a) Molina, D. A. C.; Casey, C. P.; Müller, I.; Nozaki, K.; Jäkel, C. *Organometallics* **2010**, *29*, 3362–3367. (b) Gual, A.; Godard, C.; Castillon, S.; Claver, C. *Adv. Synth. Catal.* **2010**, *352*, 463–477. (c) van der Veen, L. A.; Keeven, P. H.; Schoemaker, G. C.; Reek, J. H. N.; Kamer, P. C. J.; van Leeuwen, P. W. N. M.; Lutz, M.; Spek, A. L. *Organometallics* **2000**, *19*, 872–883. (d) van der Veen, L. A.; Boele, M. D. K.; Bregman, F. R.; Kamer, P. C. J.; van Leeuwen, P. W. N. M.; Goubitz, K.; Fraanje, J.; Schenk, H.; Bo, C. *J. Am. Chem. Soc.* **1998**, *120*, 11616–11626. (e) Casey, C. P.; Paulsen, E. L.; Buettenueller, E. W.; Proft, B. R.; Petrovich, L. M.; Matter, B. A.; Powell, D. R. *J. Am. Chem. Soc.* **1997**, *119*, 11817–11825.

(33) For high-pressure IR studies, see: (a) Kamer, P. C. J.; van Rooy, A.; Schoemaker, G. C.; van Leeuwen, P. W. N. M. *Coord. Chem. Rev.* **2004**, *248*, 2409–2424. (b) Kubis, C.; Ludwig, R.; Sawall, M.; Neymeyr, K.; Borner, A.; Wiese, K. D.; Hess, D.; Franke, R.; Selent, D. *ChemCatChem* **2010**, *2*, 287–295. (c) Diebolt, O.; van Leeuwen, P. W. N. M.; Kamer, P. C. J. *ACS Catal.* **2012**, *2*, 2357–2370.

(34) For details, see the SI.

(35) Blackmond, D. G. *Angew. Chem., Int. Ed.* **2005**, *44*, 4302–4320.

(36) Inhibition effect of various carboxylic acids on the hydroformylation of 1-hexene has already been reported, and the study showed the more pronounced effect for more acidic benzoic acid derivatives, see: (a) Mieczynska, E.; Trzeciak, A. M.; Ziolkowski, J. J. *Mol. Catal.* **1993**, *80*, 189–200. See also: (b) Varshavskii, Y. S.; Cherkasova, T. G.; Podkorytov, I. S.; Korlyukov, A. A.; Khrustalev, V. N.; Nikol’skii, A. B. *Russ. J. Coord. Chem.* **2005**, *31*, 121–131.

(37) To characterize further the influence of the product on the catalyst stability, we performed an additional experiment with the prolonged catalyst incubation (20 h) in the presence of the product, followed by substrate addition. In this case, the observed reaction rate was about three times lower compared to experiments in which the precatalyst was first activated in the absence of any acid, prior to the addition of the mixture of the substrate and the product (SI Figure S39). This shows that in the first experiment, two-thirds of the catalyst got deactivated involving the presence of the product during the incubation period of 20 h, and hence the catalyst half-lifetime under these conditions is $t_{1/2} \approx 13$ h. Similarly, precatalyst activation in the presence of 4-heptylbenzoic acid results in the same level of catalyst deactivation (SI Figure S39). As the catalyst is stable in the absence of any carboxylate-containing compounds (>24 h), the deactivation process likely involves also a carboxylate group of the product molecule. Furthermore, a kinetic experiment under more challenging conditions, that is at elevated temperature and with a very low catalyst loading of 0.001 mol% Rh (substrate to catalyst ratio of 100 000:1) shows that initially the reaction proceeds with a remarkable turnover frequency of 18 000 mol mol⁻¹ h⁻¹ (5 turnovers per second!).

However, after performing 44 000 turnovers, the catalyst is fully deactivated, and the reaction stops (SI Figure S40). Importantly, prior to that, the catalyst is highly active, allowing for high catalyst efficiency, which is crucial in view of commercial applications.

(38) Copeland, R. A. *Enzymes: A Practical Introduction to Structure, Mechanism, and Data Analysis*; Wiley-VCH: New York, 2000.

(39) A similar experiment for phosphine ligand **L1** in the presence of product **8** shows formation of the typical rhodium hydride species, $[\text{Rh}(\text{L1})(\text{CO})_2\text{H}]$ —the same complex as in the absence of **8** (in line with the previous study for aliphatic carboxylic acids) (ref 18b). The relatively high electrophilicity of the rhodium center of phosphite-based complexes, compared with phosphine-based complexes, seems crucial for promoting the coordination of carboxylates to the rhodium center.

(40) (a) Caporali, M.; Frediani, P.; Salvini, A.; Laurenczy, G. *Inorg. Chim. Acta* **2004**, 357, 4537–4543. (b) Zhang, J.; Poliakoff, M.; George, M. W. *Organometallics* **2003**, 22, 1612–1618. (c) Kubis, C.; Selent, D.; Sawall, M.; Ludwig, R.; Neymeyr, K.; Baumann, W.; Franke, R.; Börner, A. *Chem.—Eur. J.* **2012**, 18, 8780–8794. (d) van der Slot, S. C.; Kamer, P. C. J.; van Leeuwen, P. W. N. M.; Iggo, J. A.; Heaton, B. T. *Organometallics* **2001**, 20, 430–441. (e) Brown, J. M.; Kent, A. G. *J. Chem. Soc., Perkin Trans. 2* **1987**, 1597–1607.